

Design of Near-Infrared Dyes Based on π -Conjugation System Extension 2. Theoretical Elucidation of Framework Extended Derivatives of Perylene Chromophore

Masafumi Adachi*[†] and Yukinori Nagao[‡]

Mitsubishi Chemical Corporation, Yokohama Research Center, 1000 Kamoshida-cho, Aoba-ku, Yokohama 227-8502, Japan, and Faculty of Science and Technology, Science University of Tokyo, 2641 Yamazaki, Noda 278-8510, Japan

Received October 26, 2000. Revised Manuscript Received December 4, 2000

To design near-infrared (NIR) absorbing polyaromatic dyes, we have theoretically elucidated the electronic transition properties of the extended π -conjugation derivatives of 3,4,9,10-perylenetetracarboxylic dianhydride diimide (PTCAI). Framework extension along the molecular long axis, that is, to terylene (TTCAl) and quaterylene (QTCAI), causes a large bathochromic shift by the narrowing of the HOMO–LUMO gap. Despite the larger π -conjugation, framework expansion along the molecular short axis, that is, to benzo[*g,h,i*]perylene (bPTCAI) and coronene (CTCAI), causes a hypsochromic shift. Framework extension along the molecular long axis is a beneficial guiding principle of the NIR dye design. To design new polyaromatic chromophores, although the electronic transition properties are roughly determined by the core aromatic structure, we must consider the whole molecule because the modified part plays an important role in controlling the advanced properties.

1. Introduction

Near-infrared (NIR) absorbing materials (e.g., dyes and pigments) have been intensively investigated in view of their importance as the key component in optoelectronic devices.¹ However, most NIR materials are of insufficient stability (for light, heat, oxidation, etc.); therefore, only a few can be used in commercial applications. Polyaromatic hydrocarbons (PAHs) are generally stable under severe conditions and their electronic transitions, for example, absorption, fluorescence, and phosphorescence spectra, show intense response to ultraviolet and/or visible (UV–vis) light owing to their condensed π -conjugations.² Therefore, PAHs have been applied to chromogens (dyes, pigments, and fluorescent materials).^{2f,g,i,j} But the electronic transition

properties of such chromophores have been less sufficiently elucidated than those of their parent PAHs and other kinds of chromophores (e.g., azo dye) because the solubility of PAH chromophores is generally too low because of the strong intermolecular interaction between their large planar π -systems.

3,4,9,10-Perylenetetracarboxylic dianhydride and its imide derivatives (PTCAIs, simply called a perylene or a perylene chromophore in some cases) are a typical PAH colorant.³ PTCAIs have been widely used in practical applications owing to their low light and thermal fading rates, high luminescence efficiency, and optoelectronic properties.⁴ For example, they have been used as industrial pigments,^{4b,e} laser dyes,^{4g} photoreceptors of copiers,^{4c} solar cells,^{4d} and so on. However, PTCAIs cannot absorb NIR light, even in the solid state

* To whom correspondence should be addressed. E-mail: ada@rc.mitsubishichem.co.jp. Fax: +81-45-963-3978.

[†] Mitsubishi Chemical Corporation.

[‡] Science University of Tokyo.

(1) (a) Daehne, S.; Resch-Genger, U.; Wolfbeis, O. S., Eds. *Near-Infrared Dyes for High Technology Applications*; Kluwer Academic Publishers: Dordrecht, 1998. (b) Fabian, J.; Nakazumi, H.; Matsuoka, M. *Chem. Rev.* **1992**, *92*, 1197. (c) Law, K.-Y. *Chem. Rev.* **1993**, *93*, 449. (d) Peng, Z.; Geise, H. J. *Bull. Soc. Chim. Belg.* **1996**, *105*, 739. (e) Burkinshaw, S. M.; Hallas, G.; Towns, A. D. *Rev. Prog. Coloration* **1996**, *26*, 47.

(2) (a) Vo-Dinh, T., Ed. *Chemical Analysis Vol. 101, Chemical Analysis of Polycyclic Aromatic Compounds*; John Wiley & Sons: New York, 1988. (b) Platt, J. R. *J. Chem. Phys.* **1949**, *17*, 484. (c) Clar, E.; Robertson, J. M.; Schlögl, R.; Schmidt, W. *J. Am. Chem. Soc.* **1981**, *103*, 1320. (d) Sakai, K.; Ohshima, S.; Uchida, A.; Oonishi, I.; Fujisawa, S.; Nagashima, U. *J. Phys. Chem.* **1995**, *99*, 5909. (e) Hiruta, K.; Tokita, S.; Nishimoto, K. *J. Chem. Soc., Perkin Trans. 2* **1995**, 1443. (f) Hiruta, K.; Tokita, S.; Nishimoto, K. *Dyes Pigm.* **1996**, *31*, 309. (g) Hiruta, K.; Tokita, S.; Nishimoto, K. *Dyes Pigm.* **1997**, *34*, 273. (h) Marczyk, J.; Fetzer, J. C.; Szubiakowski, J.; Waluk, J. *J. Lumin.* **1997**, *72–74*, 517. (i) Hiruta, K.; Tokita, S.; Nishimoto, K. *Dyes Pigm.* **1998**, *36*, 111. (j) Hiruta, K.; Tokita, S.; Nishimoto, K. *Dyes Pigm.* **1998**, *38*, 165.

(3) (a) Rademacher, A.; Märkle, S.; Langhals, H. *Chem. Ber.* **1982**, *115*, 2927. (b) Langhals, H. *Chem. Ber.* **1985**, *118*, 4641. (c) Demmig, S.; Langhals, H. *Chem. Ber.* **1988**, *121*, 225. (d) Ebeid, El-Z. M.; El-Daly, S. A.; Langhals, H. *J. Phys. Chem.* **1988**, *92*, 4565. (e) Langhals, H.; Fünfschilling, J.; Glatz, D.; Zschokke-Gränacher, I. *Spectrochim. Acta* **1988**, *44A*, 311. (f) Langhals, H.; Demmig, S.; Huber, H. *Spectrochim. Acta* **1988**, *44A*, 1189. (g) Kaiser, H.; Lindner, J.; Langhals, H. *Chem. Ber.* **1991**, *124*, 529. (h) Johansson, L. B.-Å.; Langhals, H. *Spectrochim. Acta* **1991**, *47A*, 857. (i) Deligeorgiev, T.; Zaneva, D.; Petkov, I.; Timcheva, I.; Sabnis, R. *Dyes Pigm.* **1994**, *24*, 75. (j) Adachi, M.; Murata, Y.; Nakamura, S. *J. Phys. Chem.* **1995**, *99*, 14240. (k) Mercadante, R.; Trsic, M.; Duff, J.; Aroca, R. *J. Mol. Struct. (THEOCHEM)* **1997**, *394*, 215.

(4) (a) Krasovitskii, B. M.; Bolotin, B. M. *Organic Luminescent Materials*; VCH: Weinheim, 1988. (b) Herbst, W.; Hunger, K. *Industrial Organic Pigments. Second Ed.*; VCH: Weinheim, 1997. (c) Popovic, Z. D.; Loutfy, R. O.; Hor, Ah-M. *Can. J. Chem.* **1985**, *63*, 134. (d) Panayotatos, P.; Parikh, D.; Sauer, R.; Bird, G.; Piechowski, A.; Husain, S. *Solar Cells* **1986**, *18*, 71. (e) Klebe, G.; Graser, F.; Hädicke, E.; Berndt, J. *Acta Crystallogr.* **1989**, *B45*, 69. (f) Seybold, G.; Wagenblast, G. *Dyes Pigm.* **1989**, *11*, 303. (g) Sadrai, M.; Hadel, L.; Sauer, R. R.; Husain, S.; Krogh-Jespersen, K.; Westbrook, J. D.; Bird, G. R. *J. Phys. Chem.* **1992**, *96*, 7988.

(as pigments).^{3,4} Therefore, the NIR absorbing dye, keeping such excellent properties, has been strongly required.

Most NIR dyes have been designed based on the conventional understanding that "Larger π -conjugation causes a bathochromic shift". But this is not always true;⁵ for example, the quinone ring extension of indoniline dyes causes a hypsochromic shift.⁶ Even though many such exceptions have been known, the above methodology is still efficient under limited conditions; therefore, we must first fully understand the characteristics of the current system and then design new chromophores based on a suitable principle. Theoretical analyses of chromophores provide a basic understanding of their electronic transition properties as well as the requisite information to design new colorants, for example, those that absorb and/or emit desirable light.⁵ We have theoretically elucidated the PAH dyes focused on the relationship between their π -conjugations and electronic transition properties (UV-vis absorption spectrum) by using the semiempirical INDO/S⁷ molecular orbital (MO) method with the molecular structure optimization by the AM1⁸ method.^{3j,9} First, we analyzed the PTCAI electronic transition properties based on the characteristics of the fragments.^{3j} In a preceding paper (part 1 of this study),⁹ we analyzed the arylimidazole introduction effect into the perylene chromophore and concluded that, although this modification causes a bathochromic shift, this shift is insufficient to realize NIR absorbing dyes. These results clearly indicate the importance of theoretical analysis for the design of new PAH chromophores.

There are two ways of extending the π -conjugation of the perylene chromophore; one is extension of the perylene framework¹⁰ and the other is arylimidazole introduction.¹¹ Recently, these modified dyes have been actively investigated by our,^{10m,11a,b,d,12} Müllen's,^{10c,e-k,11i} and Langhals'^{10d,l,11c,h} groups and these electronic tran-

sition properties (e.g., absorption and fluorescence spectra) have been reported. Synthesis of the perylene mainframe extended PTCAI analogues is a recent topic in photofunctional materials research.^{10,12} In 1991, we tried to synthesize the quaterylene-type analogue, but the final annulation between two perylene moieties was unsuccessful.¹² Four years later, Müllen's group succeeded in synthesizing the quaterlylenetetra-carboxylic dianhydride diimide (QTCAI) dyes and reported their absorption spectra.^{10c} Later, Langhals'^{10d} and our^{10m} groups also synthesized QTCAI and observed their properties. Müllen's and Langhals' groups have actively synthesized new dyes constructed from various annulated cores by selecting exquisite synthesis routes; recently, they synthesized the terrylene,^{10e} coronene,^{10h} and benzo[*g,h,i*]perylene^{10l} analogues and elucidated their absorption and fluorescence spectra and other optical properties.^{10c-1} In this study, we theoretically analyze the perylene framework extension to evaluate the possibility of NIR dye design because the shift by the arylimidazole introduction is insufficient to realize NIR absorbing dyes.⁹

2. Calculation Method

We analyzed the absorption spectra of 3,4,9,10-perylenetetra-carboxylic dianhydride diimide (PTCAI) and its terrylene (TTCAI), quaterylene (QTCAI), coronene (CTCAI), and benzo[*g,h,i*]perylene (bPTCAI) analogous dyes (Chart 1) by MO calculations. In the calculations, we selected the H atom as their imide substituent because the imide substituents do not affect the absorption spectrum.^{3j,13}

In the first step, the molecular structures were optimized by the AM1 method⁸ using the MOPAC program package.¹⁴ We calculated the geometries, disregarding the usual restriction of the planarity, but all optimized structures were nearly planar. The equilibrium structures were then employed in the second step to calculate the absorption spectra by the INDO/S method.⁷ In this method, which is a modified INDO version for absorption spectrum calculations, integrals were evaluated with the Nishimoto-Mataga formula,¹⁵ and SCF calculations were executed at the closed-shell Hatree-Fock level (RHF). Configuration interaction (CI) calculations were performed to include single excited configurations from the ground state, consisting of 35 (occupied orbitals) \times 35 (virtual orbitals) configurations.

3. Results and Discussion

A. π -Conjugation Extension along the Molecular Long Axis. When the π -conjugation is extended along the molecular long axis from PTCAI to TTCAI and QTCAI, the observed absorption maximum (λ_{\max}) of

(5) (a) Orchin, M.; Jaffé, H. H. *Symmetry, Orbitals, and Spectra*; John Wiley & Sons: New York, 1971. (b) Griffiths, J. *Colour and Constitution of Organic Molecules*; Academic: London, 1976. (c) Fabian, J.; Hartmann, H. *Light Absorption of Organic Colorants*; Springer: Berlin, 1980. (d) Zollinger, H. *Color Chemistry. Second Ed.*; VCH: Weinheim, 1991.

(6) Adachi, M.; Murata, Y. *J. Phys. Chem. A* **1998**, *102*, 841.

(7) (a) Ridley, J.; Zerner, M. *Theor. Chim. Acta* **1973**, *32*, 111. (b) Ridley, J. E.; Zerner, M. C. *Theor. Chim. Acta* **1976**, *42*, 223. (c) Bacon, A. D.; Zerner, M. C. *Theor. Chim. Acta* **1979**, *53*, 21. (d) Zerner, M. C.; Loew, G. H.; Kirchner, R. F.; Mueller-Westerhoff, U. T. *J. Am. Chem. Soc.* **1980**, *102*, 589.

(8) Dewar, M. J. S.; Zoebisch, E. G.; Healy, E. F.; Stewart, J. J. P. *J. Am. Chem. Soc.* **1985**, *107*, 3902.

(9) Adachi, M.; Nagao, Y. *Chem. Mater.* **1999**, *11*, 2107.

(10) (a) Désilets, D.; Kazmaier, P. M.; Burt, R. A. *Can. J. Chem.* **1995**, *73*, 319. (b) Désilets, D.; Kazmaier, P. M.; Burt, R. A.; Hamer, G. K. *Can. J. Chem.* **1995**, *73*, 325. (c) Quante, H.; Müllen, K. *Angew. Chem., Int. Ed. Engl.* **1995**, *34*, 1323. (d) Langhals, H.; Schönmann, G.; Feiler, L. *Tetrahedron Lett.* **1995**, *36*, 6423. (e) Holtrup, F. O.; Müller, G. R. J.; Quante, H.; De Feyter, S.; De Schryver, F. C.; Müllen, K. *Chem. Eur. J.* **1997**, *3*, 219. (f) Mais, S.; Tittel, J.; Basché, Th.; Bräuchle, C.; Göhde, W.; Fuchs, H.; Müller, G.; Müllen, K. *J. Phys. Chem. A* **1997**, *101*, 8435. (g) Göhde, W., Jr.; Fischer, U. C.; Fuchs, H.; Tittel, J.; Basché, Th.; Bräuchle, C.; Herrmann, A.; Müllen, K. *J. Phys. Chem. A* **1998**, *102*, 9109. (h) Rohr, U.; Schlichting, P.; Böhm, A.; Gross, M.; Meerholz, K.; Bräuchle, C.; Müllen, K. *Angew. Chem., Int. Ed.* **1998**, *37*, 1434. (i) Geerts, Y.; Quante, H.; Platz, H.; Mahrt, R.; Hopmeier, M.; Böhm, A.; Müllen, K. *J. Mater. Chem.* **1998**, *8*, 2357. (j) Lee, S. K.; Zu, Y.; Herrmann, A.; Geerts, Y.; Müllen, K.; Bard, A. J. *J. Am. Chem. Soc.* **1999**, *121*, 3513. (k) Schlichting, P.; Duchscherer, B.; Seisenberger, G.; Basché, T.; Bräuchle, C.; Müllen, K. *Chem. Eur. J.* **1999**, *5*, 2388. (l) Langhals, H.; Kirner, S. *Eur. J. Org. Chem.* **2000**, 365. (m) Nagao, Y.; Takada, T.; Kozawa, K., in preparation.

(11) (a) Nagao, Y.; Ishikawa, N.; Tanabe, Y.; Misono, T. *Chem. Lett.* **1979**, 151. (b) Nagao, Y.; Ishikawa, N.; Tanabe, Y.; Misono, T. *Nippon Kagaku Kaishi* **1980**, 1391. (c) Lukác, I.; Langhals, H. *Chem. Ber.* **1983**, *116*, 3524. (d) Nagao, Y.; Misono, T. *Dyes Pigm.* **1984**, *5*, 171. (e) Popovic, Z. D.; Hor, A. M.; Loutfy, R. O. *Chem. Phys.* **1988**, *127*, 451. (f) Loutfy, R. O.; Hor, A. M.; Kazmaier, P.; Tam, M. *J. Imag. Sci.* **1989**, *33*, 151. (g) Fujita, Y.; Adachi, C.; Tsutsui, T.; Saito, S. *Nippon Kagaku Kaishi* **1992**, 1154. (h) Langhals, H.; Sprenger, S.; Brandherm, M.-T. *Liebigs Ann.* **1995**, 481. (i) Quante, H.; Geerts, Y.; Müllen, K. *Chem. Mater.* **1997**, *9*, 495.

(12) Nagao, Y.; Abe, Y.; Misono, T. *Dyes Pigm.* **1991**, *16*, 19.

(13) In contrast, the solid-state spectrum (color as the pigment) largely depends on the imide substituents because they control the intramolecular interaction and determine the crystal packing; for example, see ref 4e.

(14) MOPAC Ver. 5, Stewart, J. J. P. *QCPE Bull.* **1989**, *9*, 10.

(15) (a) Nishimoto, K.; Mataga, N. *Z. Phys. Chem. (Neue Folge)* **1957**, *12*, 335. (b) Mataga, N.; Nishimoto, K. *Z. Phys. Chem. (Neue Folge)* **1957**, *13*, 140.

Chart 1

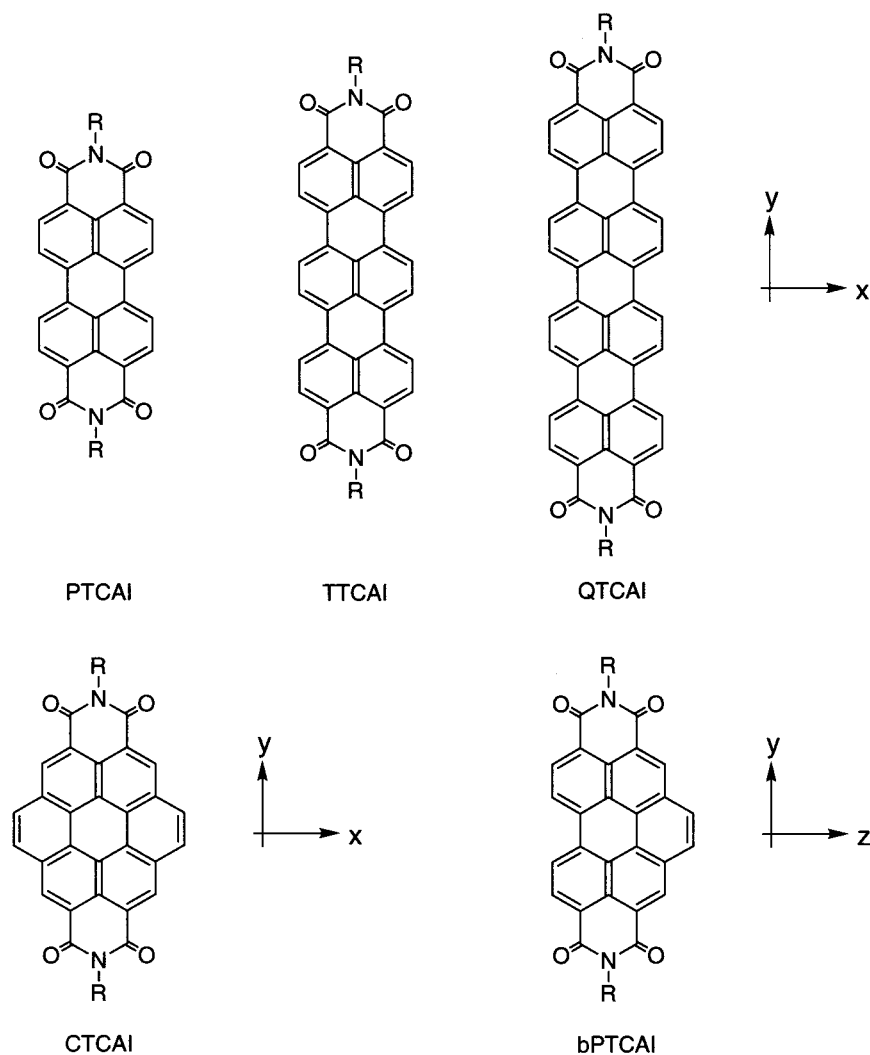


Table 1. Observed and Calculated Absorption Spectra of Polynaphthalenetetracarboxylic Dianhydride Diimide Dyes

dye ^a	observed		calculated (INDO/S)			
	λ_{\max} (nm)	ϵ_{\max}	λ_{\max} (nm)	f^b	transition property ^c	
PTCAI	526 ^d	81 500	441	1.258	$B_{2u}(y)$	-0.981{(HOMO, 70) → (LUMO, 71)}
	370	4 000	344	0.022	$B_{3u}(x)$	0.701{68 → LUMO} 0.583{HOMO → 75}
TTCAI	650 ^e	93 300	520	1.834	$B_{2u}(y)$	-0.974{(HOMO, 92) → (LUMO, 93)}
			359	0.002	$B_{3u}(x)$	0.660{HOMO → 98} -0.492{87 → LUMO} -0.352{89 → LUMO}
QTCAI	764 ^f	162 000	580	2.404	$B_{2u}(y)$	-0.961{(HOMO, 114) → (LUMO, 115)}
	375	14 700	361	0.010	$B_{3u}(x)$	0.513{HOMO → 121} -0.446{HOMO → 123} 0.434{107 → LUMO}
CTCAI	511 ^g	19 700	432	0.118	$B_{3u}(x)$	0.814{(HOMO, 78) → (LUMO, 79)}
	428	62 100	376	0.471	$B_{2u}(y)$	0.468{77 → 80} 0.887{77 → LUMO} -0.421{HOMO → 80}
bPTCAI	468 ^h	75 910	402	0.077	$A_1(z)$	0.811{73 → (LUMO, 75)}
			400	1.053	$B_2(y)$	0.415{(HOMO, 74) → 77} -0.966{HOMO → LUMO}

^a R = H, in calculation. ^b Oscillator strength. ^c Excitations having the CI coefficient over 0.3 are shown. ^d R = 2-ethylhexyl, in CHCl₃ solution, ref 3j. ^e R = 2,6-di(isopropyl)phenyl, in CHCl₃ solution, ref 10e. ^f R = 2,6-di(isopropyl)phenyl, in CH₂Cl₂ solution, ref 10c. ^g R = cyclohexyl, 3,9-didecyl on coronene framework, in CH₂Cl₂ solution, ref 10h. ^h R = 1-hexylheptyl, in CHCl₃ solution, ref 10l.

their main-band is largely shifted to a longer wavelength (bathochromic shift) to the NIR region (Table 1). The calculated main-band (B_{2u} , polarized toward the molec-

ular long y -axis), which is mainly characterized as HOMO → LUMO excitation, roughly reproduces this observed bathochromic shift (Table 1).¹⁶

Table 2. Detail of HOMO → LUMO Excitation Properties of Polynaphthalenetetracarboxylic Dianhydride Diimide Dyes (INDO/S)

dye ^a	transition energy ^b (cm ⁻¹)	¹ E _{HOMO→LUMO} ^c (cm ⁻¹)	Δε _{HOMO,LUMO} ^d (cm ⁻¹)	J _{HOMO,LUMO} ^e (cm ⁻¹)	2K _{HOMO,LUMO} ^f (cm ⁻¹)	J - 2K (cm ⁻¹)	ε _{HOMO} ^g (au)	ε _{LUMO} ^g (au)
PTCAI	22 660	23 970	44 530	28 860	8300	20 560	-0.29 088	-0.08 800
TTCAI	19 230	20 600	39 380	25 460	6680	18 780	-0.26 714	-0.08 770
QTCAI	17 250	18 850	36 390	23 020	5480	17 540	-0.25 262	-0.08 683
CTCAI	23 120 ^h	27 380	48 100	26 460	5740	20 720	-0.29 473	-0.07 559
	26 590 ⁱ	29 170	49 470	27 290	6990	20 300	-0.30 097	-0.07 559
bPTCAI	25 010	26 620	47 090	27 970	7500	20 470	-0.29 588	-0.08 130

^a R = H, in calculation. ^b Energy expression of the λ_{max}. ^c Singlet excitation energy. ^d Difference of orbital energies. ^e Coulomb integral. ^f Exchange integral. ^g Orbital energy. ^h B_{3u} transition (432 nm). ⁱ B_{2u} transition (376 nm), this row shows the (77th orbital) → LUMO excitation property.

Singlet HOMO → LUMO excitation energy (¹E_{HOMO→LUMO}) is expressed by using the orbital gap and electronic interaction terms *J* and *K*:

$${}^1E_{\text{HOMO}\rightarrow\text{LUMO}} = \Delta\epsilon_{\text{HOMO,LUMO}} - J_{\text{HOMO,LUMO}} + 2K_{\text{HOMO,LUMO}} \quad (1)$$

(Δε, HOMO–LUMO energy gap;
J, Coulomb integral; *K*, exchange integral)

Each component of the ¹E_{HOMO→LUMO} is summarized in Table 2. When the π-conjugation is extended, both the HOMO → LUMO excitation energy and the HOMO–LUMO gap largely decline, but the latter change is larger than the former decrease. In contrast, the electronic interaction term (*J* - 2*K*) contributes to a slight increase of the HOMO → LUMO excitation energy (Table 2 and eq 1).¹⁷ Therefore, this bathochromic shift originates from the narrowing HOMO–LUMO gap and ought to be explained by the HOMO and LUMO energy levels.

Figure 1 illustrates HOMOs and LUMOs of PTCAI, TTCAI, and QTCAI with their energy levels. With extension of the π-conjugation along the molecular long axis, the HOMO level rises; on the other hand, the LUMO level is scarcely affected. Therefore, the HOMO behavior is the main reason for this bathochromic shift.

B. Mechanism of Orbital Energy Shift. Figure 2 illustrates a correlation diagram of the molecular orbitals between PTCAI, TTCAI, and QTCAI. When the π-conjugation is extended along the molecular long axis, these orbitals split into the same number as their naphthalene moieties. First, we consider the QTCAI orbitals originating from naphthalene HOMO (103rd, 111th, 113th, and 114th). In the most stable orbital (103rd, b_{2g}), all bridges between each naphthalene fragment are characterized as the bonding connections

(16) Not limited to the INDO/S method, conventional semiempirical MO calculations underestimate the absorption wavelength, especially for organic dyes and pigments. Because the parameter sets are determined to reproduce the transitions of small aromatic molecules (e.g., benzene), this disagreement increases with extending the π-conjugation. From the theoretical viewpoint, this behavior is due to the unbalanced count of one- and two-electron parts in the electronic transition energy. Nishimoto, K. *Bull. Chem. Soc. Jpn.* **1993**, *66*, 1876. Although such an underestimation appears in the INDO/S calculation, the discrepancy from the observation can be approximately expressed by a linear correlation; therefore, we have previously proposed the relationship between the observed and INDO/S calculated λ_{max}: λ_{max}(obs) = 1.65 λ_{max}(calc) - 187 (nm). Adachi, M.; Nakamura, S. *Dyes Pigm.* **1991**, *17*, 287. By using this correction, we can obtain reasonable λ_{max} values (e.g., PTCAI, 541 nm; TTCAI, 671 nm; QTCAI, 770 nm).

(17) Extension of the π-conjugation causes slight reduction of the electronic interaction term (*J* - 2*K*) by decreasing the Coulomb interaction because the HOMO and LUMO delocalize in the whole molecule (Figure 1).

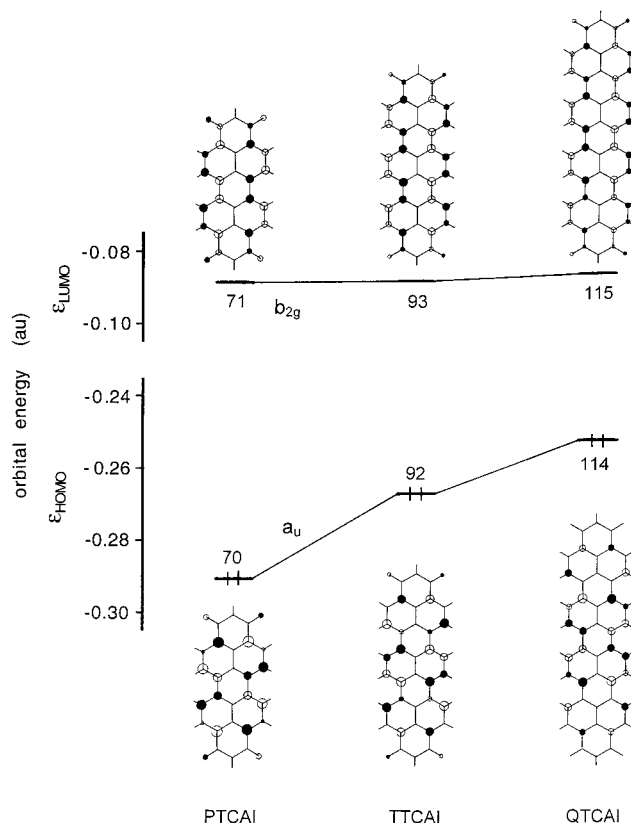


Figure 1. HOMOs and LUMOs of polynaphthalenetetracarboxylic dianhydride diimide dyes (INDO/S).

(Figure 3). Antibonding connections appear in the next stable orbital (111th, a_u) at the center of the molecule. The orbital stability decreases by increasing the number of antibonding connections; moreover, these orbitals largely split in the energy (Figures 1–3). All bridges in the HOMO are characterized as the antibonding connections; therefore, the π-conjugation extension causes elevation of the HOMO level by an increase of the antibonding interaction (Figure 1).

On the other hand, the LUMO (115th, b_{2g}) of QTCAI is roughly characterized as four naphthalene LUMOs; all are bridged by the bonding connections (Figure 1). When the stability is decreased (to 116th, 117th, and 124th), these bridges reverse the antibonding property, step by step (see 116th orbital in Figure 3). In contrast to the HOMO, the LUMO level is not affected by the lengthening π-conjugation because all bridges are always the bonding connections (Figure 1).¹⁸ As a result, the π-conjugation extension along the molecular long axis causes the bathochromic shift by the HOMO–LUMO gap reduction.

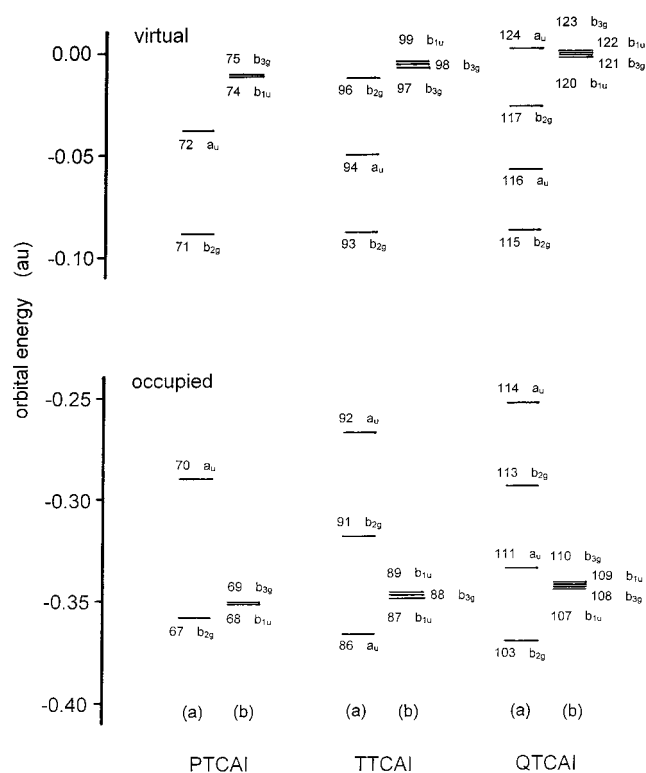


Figure 2. Orbital energy diagram of polynaphthalenetetracarboxylic dianhydride diimide dyes (INDO/S): (a) originating from naphthalene HOMO and LUMO; (b) originating from naphthalene next HOMO and next LUMO.

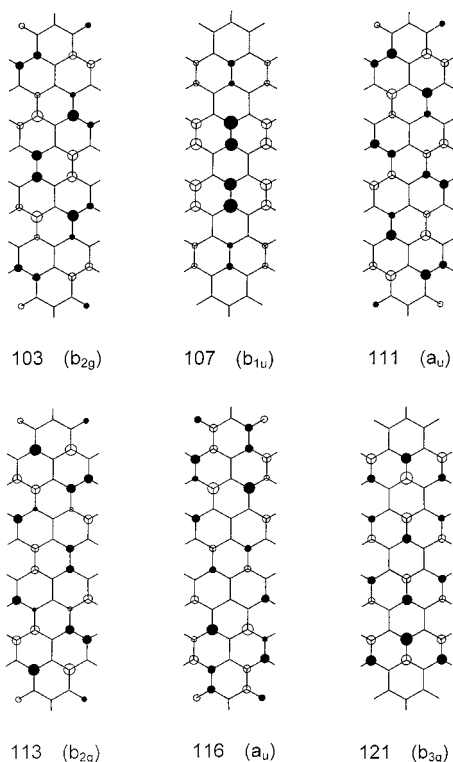


Figure 3. Molecular orbitals of QTCAI (INDO/S).

C. Comparison of Absorption Spectra: PTCAI, TTCAI, and QTCAI. The calculated absorption spectra, including sub-bands, of PTCAI, TTCAI, and QTCAI are summarized in Table 3. When the π -conjugation is extended along the molecular long axis, the intense longest transition (B_{2u} , main-band) shows a large ba-

Table 3. Calculated Absorption Spectra of Polynaphthalenetetracarboxylic Dianhydride Diimide Dyes^a(INDO/S)

PTCAI		TTCAI		QTCAI		transition property
λ_{\max} (nm)	f^b	λ_{\max} (nm)	f^b	λ_{\max} (nm)	f^b	
441	1.258	520	1.834	580	2.404	B_{2u} (y, main-band) ^c
		374	0.000	421	0.000	A_g^c
		357	0.000	374	0.000	B_{1g}^c
				369	0.000	A_g^c
347	0.000	349	0.000	363	0.000	B_{1g}^d
344	0.022	359	0.002	361	0.010	B_{3u} (x, sub-band) ^d
<i>e</i>		301	0.080	341	0.101	B_{2u} (y) ^c

^a R = H, in calculation. ^b Oscillator strength. ^c Corresponds to the naphthalene B_{2u} (1L_a) transition. ^d Corresponds to the naphthalene B_{3u} (1L_b) transition. ^e Shorter than 250 nm.

thochromic shift with strengthening of its intensity. On the other hand, the weakly intense sub-transition (B_{3u}) is shifted to only slightly bathochromic (PTCAI, 344 nm; TTCAI, 359 nm; QTCAI, 361 nm). The orbitals originating from naphthalene next HOMO (HOMO-1 orbital) and next LUMO (LUMO+1 orbital) play an important role in this sub-transition (Table 1 and Figure 2b). In these orbitals, the bridging points (1-, 4-, 5-, and 8-positions on the naphthalene ring) contribute to neither bonding characteristic (see 107th and 121st orbitals in Figure 3); therefore, the π -conjugation size scarcely affects these orbital levels (Figure 2b), and moreover, the transition energy of the sub-band. In other words, the π -conjugation of the sub-transition (polarized toward the *x*-axis, see Chart 1) is the same as that of the naphthalene B_{3u} (1L_b) transition on all dyes; therefore, the absorption property scarcely changes.

The calculated main-band of further extended polynaphthalenetetracarboxylic dianhydride diimide dyes shows a more bathochromic shift with strengthening of its intensity (pentarylene, 624 nm (f 2.924); hexarylene, 659 nm (f 3.425); heptarylene, 687 nm (f 3.924); octarylene, 711 nm (f 4.412)) because the longer π -conjugation causes unstabilization of the HOMO level (see section 3B) and an increase of the transition dipole length.¹⁹ Although the INDO/S calculation systematically underestimates the λ_{\max} to be shorter than the observed value, we can use it for prediction through appropriate correction;¹⁶ therefore, these results clearly show that we can design the tailored NIR, and moreover, IR absorbing PAH dyes by the suitable π -conjugation extension.

NIR (and/or IR) absorbing materials without visible color (i.e., no absorption in the human visible region) have been strongly required for many applications, for example, a heat radiation sealant, a security print

(18) By extension of the π -conjugation, the lowest orbital originating from naphthalene HOMO is slightly stabilized by the increase of the average bonding property (at one naphthalene moiety) because the bridges between the naphthalene and carboxylic moieties do not contribute to any bonding properties (Figures 2 and 3). In contrast, such an average property of the LUMO does not change since the corresponding bridges are already bonding connections (Figure 1); therefore, the LUMO level is almost the same.

(19) With an increase in the number of naphthalene rings, the change in the transition energy reduces in agreement with the general theory and experimental results (see ref 5); in other words, there is a limit of the bathochromic shift. Therefore, we can only design new dyes under such a limited absorption wavelength.

Table 4. Calculated Absorption Properties of Coronene and CTCAI (INDO/S)

coronene				CTCAI ^a			
λ_{\max} (nm)	f^b	transition properties ^c		λ_{\max} (nm)	f^b	transition properties ^c	
404	0.000	B _{2u}	-0.682{53 → 56} -0.682{(HOMO, 54) → (LUMO, 55)}	432	0.118	B _{3u} (x)	0.841{(HOMO, 78) → (LUMO, 79)} 0.468{77 → 80}
349	0.000	B _{1u}	0.698{53 → LUMO} -0.698{HOMO → 56}	376	0.471	B _{2u} (y)	0.887{77 → LUMO} -0.421{HOMO → 80}
290 ^d	1.964	E _{1u} (x, y)	-0.594{53 → LUMO} -0.594{HOMO → 56} -0.349{53 → 56} 0.349{HOMO → LUMO}	303	2.126	B _{2u} (y)	-0.876{HOMO → 80} -0.401{77 → LUMO}
290 ^d	1.964	E _{1u} (x, y)	0.594{53 → 56} -0.594{HOMO → LUMO} -0.349{53 → LUMO} -0.349{HOMO → 56}	299	1.218	B _{3u} (x)	-0.824{77 → 80} 0.486{HOMO → LUMO}

^a R = H, in calculation. ^b Oscillator strength. ^c Excitations having the CI coefficient over 0.3 are shown. ^d Observed: 331 nm at gas phase, ref 22a.

system, and so forth, but practical materials are scarcely known.¹ On the basis of the knowledge concerning the main- and sub-transition properties, we should assume that we can design colorless NIR and/or IR dyes by the adjusted π -conjugation extension. But before concluding this possibility, we must carefully analyze in detail the properties of other transitions.²⁰ We should focus on a new allowed B_{2u} transition lying in a UV region (bottom row in Table 3, TTCAI 301 nm, QTCAI 341 nm).²¹ This B_{2u} transition is characterized as the excitation between naphthalene HOMO and LUMO originated orbitals, that is, from the next HOMO (b_{2g}) to the next LUMO (a_u: TTCAI 91st → 94th, QTCAI 113th → 116th, Figures 2a and 3). π -Conjugation extension along the molecular long axis causes the unstabilization of the next HOMO level and the approach of the next LUMO level to that of the LUMO (Figure 2a); as a result, this B_{2u} transition is shifted to a longer wavelength. In conclusion, we can get the PAH NIR, moreover IR absorbing dyes, but these dyes might have more or less visual color.

D. π -Conjugation Expansion along the Molecular Short Axis. The observed absorption spectrum of CTCAI is strange (Table 1); despite the larger π -conjugation, the longest absorption band (511 nm, ϵ 19700) shows a slight hypsochromic shift from PTCAI's (526 nm, ϵ 81500) with weakened intensity, and a new intense band appears in the shorter wavelength (428 nm, ϵ 62100).^{10h} The theoretical calculation clearly reproduces such novel behavior (Table 1). We should note that the CTCAI's lowest energy band is a B_{3u} transition (polarized toward the molecular short x -axis) and the next band is a B_{2u} transition (y -axis); these polarized directions are opposite those of the PTCAI's main- and sub-transitions. Such evidence strongly suggests that CTCAI is not a simple analogue of PTCAI. Therefore, first of all, we will consider the transition properties of CTCAI by comparison with those of the core coronene fragment.

(20) On all dyes, four negligibly intense $n-\pi^*$ transitions, characterized as the excitations from the lone pair orbitals of the carbonyl O atoms to virtual orbitals, lie in the 348–373-nm region. Perylene framework extension only slightly shifts these transitions because the properties of such n orbitals (energy levels and shapes) are scarcely affected.

(21) A similar B_{2u} transition, mainly characterized as the 67th → 72nd orbitals excitation, should also appear on PTCAI. But this band lies in an extremely high energy region (shorter than 250 nm); therefore, it was not calculated.

Details of the calculated transition properties of coronene and CTCAI with their correspondence are summarized in Table 4. The correlation diagram of the frontier molecular orbitals between coronene and CTCAI is drawn in Figure 4; HOMO and next HOMO of CTCAI correspond to each one of the coronene HOMOs, and the coronene LUMOs counterparts are CTCAI's LUMO and next LUMO. Coronene can be regarded as the expanded molecule of the benzene π -conjugation; therefore, its electronic transitions are similar to those of benzene; two forbidden transitions (B_{2u}, 404 nm; B_{1u}, 349 nm) and degenerate allowed transitions (E_{1u}, 290 nm) appear from the degenerate coronene's HOMOs (e_{2u}) and LUMOs (e_{1g}).²² The lowest energy CTCAI transition (B_{3u}) corresponds to the coronene forbidden B_{2u} transition. Moreover, the π -conjugation polarized toward this transition is the same as that of coronene (x -direction, see Chart 1); therefore, this absorption intensity is small. The CTCAI next transition (B_{2u}) corresponds to the coronene forbidden B_{1u} transition, but the π -conjugation along the y -axis is largely modified from that of the coronene by the tetracarboxylic dianhydride diimide introduction; as a result, this band has middle intensity. On the other hand, both observed 338 nm (ϵ 73200) and 334 nm (ϵ 72800) bands,^{10h} corresponding to the calculated B_{2u} (303 nm, f 2.126) and B_{3u} (299 nm, f 1.218) transitions, indicate strong intensity because these originate from the intense coronene transitions (E_{1u}: 290 nm, f 1.964, Table 4).

These results clearly show that the CTCAI transitions ought to be considered as those of the coronene derivative, but the correspondence between CTCAI and PTCAI transitions has remained as an important question. Therefore, we considered the intermediate π -conjugated molecule, that is, benzo[*g,h,i*]perylene-tetracarboxylic dianhydride diimide dye (bPTCAI). The calculated intense main-band of bPTCAI (B₂: 400 nm, f 1.053) shows the hypsochromic shift from PTCAI, while the sub-band (A₁: 402 nm, f 0.077) is shifted to the longer wavelength (Table 1).²³ These calculated spectra are consistent with the observation.^{10l} The correlation dia-

(22) The calculated transition properties of coronene almost reproduce well the observations and the previous calculations: for example, (a) Aihara, J.; Ohno, K.; Inokuchi, H. *Bull. Chem. Soc. Jpn.* **1970**, *43*, 2435. (b) Ohno, K.; Kajiwara, T.; Inokuchi, H. *Bull. Chem. Soc. Jpn.* **1972**, *45*, 996. (c) Orlandi, G.; Zerbetto, F. *Chem. Phys.* **1988**, *123*, 175.

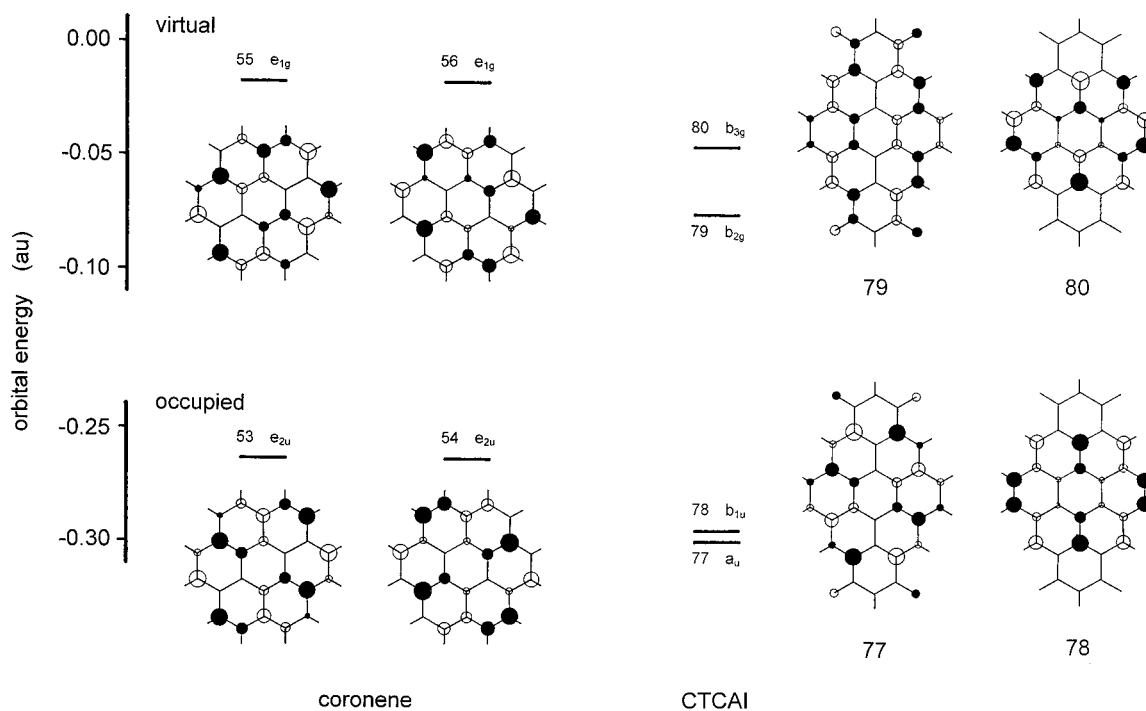


Figure 4. Correlation diagram of frontier molecular orbitals between coronene and CTCAI (INDO/S).

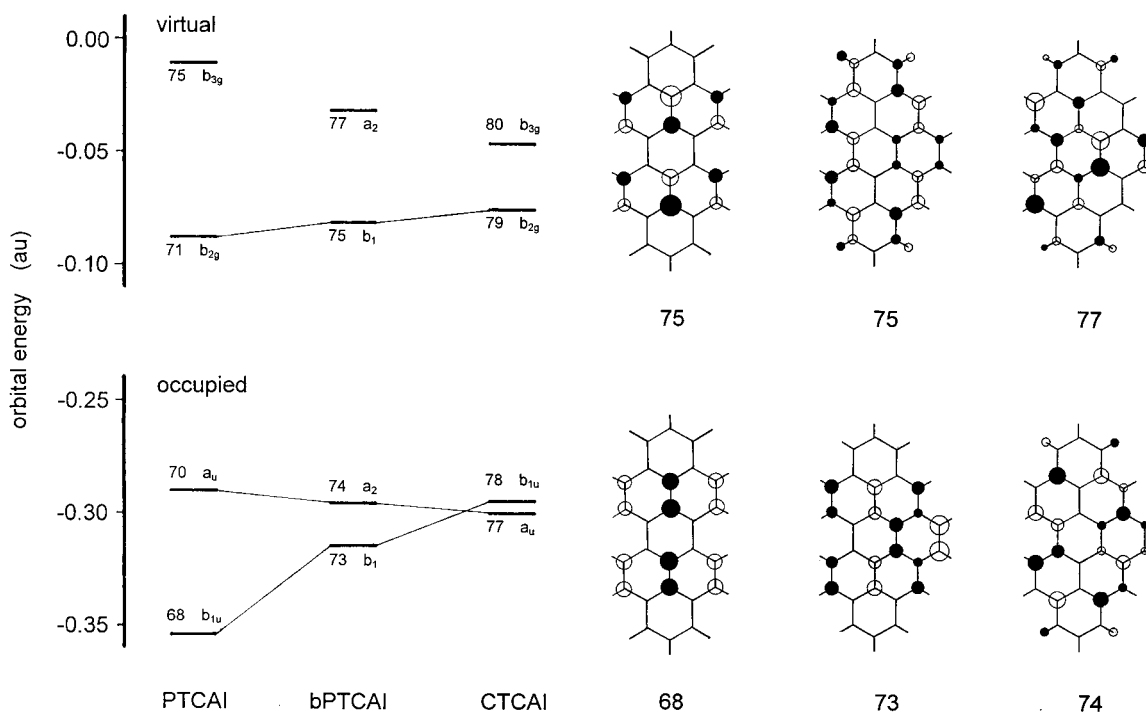


Figure 5. Correlation diagram of frontier molecular orbitals between PTCAI, bPTCAI, and CTCAI (INDO/S).

gram of the frontier molecular orbitals between PTCAI, bPTCAI, and CTCAI is drawn in Figure 5 with some important PTCAI and bPTCAI orbitals. By expansion of the π -conjugation, the correspondence of PTCAI's HOMO becomes slightly stable, and finally on CTCAI, the properties of the HOMO and next HOMO are reversed; at the same time, the LUMO level slightly rises (Figures 1, 4, and 5).²⁴ The transition property of

the main-band²⁵ can be approximately described by the excitation between these orbitals (Table 1); therefore, the widening orbital energy gap causes the hypsochromic shift because the electronic interaction is almost the same (see $J - 2K$ term in Table 2).²⁶

(24) When the π -conjugation is expanded, the number of bonding connections increases at the center of the LUMO, but the total bonding interaction reduces by shrinking the lobes of each point; therefore, the LUMO is slightly unstabilized. A little stabilization of the HOMO can be explained in the same manner.

(25) In this study, we have defined that the main-band of CTCAI is the next B_{2u} transition and the sub-band is the longest B_{3u} transition by their correspondence and intensity.

(23) On bPTCAI, the axial definition is different from that of the other molecules by its lower molecular symmetry (C_{2v} , see Chart 1). But the transitional directions of bPTCAI correspond to those of the PTCAI and CTCAI transitions.

To consider the sub-band, we analyzed the generated configurations (excitations) consisting of the sub-transition (Table 1). Expanding the π -conjugation, the important occupied orbital consisting of such excitations is largely unstabilized and such a virtual orbital is obviously stabilized (Figure 5). Therefore, the sub-band shows the large bathochromic shift because the narrowing orbital energy gap causes reduction of the excitation energies.²⁰

These results and the previous study⁹ strongly suggest that the electronic transition properties of PAH chromophores are roughly determined by their core aromatic structures and any modification, such as the tetracarboxylic dianhydride diimide and arylimidazole introductions, can be regarded as a perturbation. But, to design new chromophores, we must consider the electronic transition properties of the whole molecule because such perturbation plays an important role in determining the precise spectroscopic behavior.

4. Conclusion

To acquire the guiding principle of the NIR absorbing dye design, we have theoretically analyzed the electronic transition properties of extended π -conjugation derivatives of the perylene chromophore by using the semiempirical MO calculations. Framework extension along the

molecular long axis causes the large bathochromic shift of the main-band by the narrowing HOMO–LUMO gap, with strengthening of its intensity. On the other hand, the weak sub-band is scarcely affected because this band keeps the naphthalene B_{3u} (¹L_b) transition property. Despite the larger π -conjugation, framework expansion along the molecular short axis causes the hypsochromic shift of the main-band because this band largely reflects the transition property of its core aromatic framework rather than that of the perylene chromophore. By appropriate extension of the perylene framework, we can design the NIR and IR absorbing PAH dyes having the tailored absorption. To design the new PAH dyes, although the core aromatic structures roughly determine their characteristics, we must consider the electronic transition properties of the whole molecule because the modification plays an important role in the determination of advanced properties.

The theoretical analysis of the absorption spectrum by the INDO/S calculation with the AM1 molecular structure optimization should be an advantageous way to design new PAH chromophores. Following on the calculated results, we are advancing the synthesis of further linearly extended analogues to gain new NIR and IR absorbing dyes.

Acknowledgment. The authors thank the late Professor M. C. Zerner for the release of the ZINDO program.

CM000857V

(26) On CTCAI, the energy difference between the 77th \rightarrow LUMO and HOMO \rightarrow 80th excitations is small (4120 cm⁻¹); therefore, these excitations are mixed in the CI calculation. As a result, the transition energy largely declines from the excitation energy of its dominant configuration.